

# Estimation of Strength Properties of Some Rocks using Ball Mill Grinding Characteristics

Swamy V. Sahas, Kunar Mihir Bijay and Karra Ram Chandar\*

Department of Mining Engineering, National Institute of Technology Karnataka, Surathkal, Mangaluru-575025, INDIA

\*krc@nitk.edu.in

## Abstract

*The strength properties of rocks namely uniaxial compressive strength and tensile strength are important in design and stability evaluation of various mining, geotechnical engineering and other rock engineering projects. Accurate determination of these properties relies on high-quality samples, but challenges like sample availability, preparation of sample, cost and time constraints have led to an increasing reliance on computational methods for prediction. In this context, an indirect approach is proposed for predicting rock strength properties, specifically the uniaxial compressive strength (UCS) and tensile strength (TS), using grinding characteristics of ball mill, an unconventional yet indirect approach. A predictive modelling using multivariate regression is carried out to estimate the relationship between UCS, TS and the grinding characteristics of ball mill.*

*The developed models demonstrated high accuracy with  $R^2$  values of 0.93 for UCS and 0.96 for TS. Performance evaluation metrics showed an RMSE of 6.03 MPa and a VAF of 93.45% for UCS and an RMSE of 0.99 MPa and a VAF of 96.47% for TS. The validation was performed using experimental UCS and TS values of basalt rocks along with ball mill grinding test data. The error analysis revealed that UCS prediction error ranged from 5.1% to 11.61% while TS prediction error varied between 4.26% and 16.39%.*

**Keywords:** Ball mill, Grinding characteristics, Tensile strength, Uniaxial compressive strength.

## Introduction

In order to extract raw materials as efficiently as possible, it is imperative to evaluate the physico-mechanical properties of rocks before engaging in any rock engineering projects or mining activities. Several engineering projects require the use of rock properties such as mines, geotechnics and other engineering projects. Intact rock properties are an integral part of many rock mass classification systems as well as structures that are designed based on rock masses. This will help engineers to understand the rock formation and behavior under different conditions at a given location. Knowing the rock properties will also help in determining whether the rock is stable enough to hold the structures. The determination of rock properties such as uniaxial compressive strength, tensile strength by indirect Brazilian

tensile strength (BTS) test, shear strength, rock mass strength, elastic modulus etc. have been standardized by International Society for Rock Mechanics (ISRM)<sup>11</sup>.

Among these tests, uniaxial compressive strength (UCS) and tensile strength (TS) hold significant importance in geotechnical developments. UCS is a critical parameter for rock related engineering-based projects such as tunneling and excavation and geotechnical problems such as dam design<sup>2,7,18</sup>. Tensile strength controls the stability of the underground mines and galleries, stability of rock slopes, ability to drill and also the design of blasting in rocks<sup>15,19</sup>. High-quality core samples are necessary for the determination of these properties. However, it is sometimes difficult to obtain such specimens.

Various researchers have investigated the properties of rocks using the simple laboratory-based index tests, non-destructive tests, mineralogical characteristics, textural characteristics etc. However, the literature studies show that a limited effort is made to correlate as well as to predict the physico-mechanical properties of rocks from distinctive indirect methods such as electrical properties of rocks, crushability indices, thermal characteristics, acoustic emission characteristics, ultrasonic vibrations, grinding parameters of mills etc. Several studies in the past have been performed for predicting the physico-mechanical properties using indirect approaches. Literature studies revealed the limitations of empirical estimations of rock properties through traditional approach and also, they are less reliable and fail to explain the hidden uncertainties in the heterogenous rock behavior.

Some studies have shown to correlate the grinding parameters with the material properties. One such study is conducted by Bearman et al<sup>6</sup> where the material parameters such as compressive strength, tensile strength and abrasivity are correlated with mill parameters to predict the comminution behavior during grinding. Petrakis and Komnitsas<sup>16</sup> established correlations between material properties and breakage rate parameters determined from grinding tests, highlighting the potential of using grinding data to estimate the rock properties. A correlation between Bond work index and the mechanical properties of various Saudi ores such as uniaxial compressive strength and tensile strength was investigated by Abdel<sup>1</sup>.

Kahraman et al<sup>12</sup> evaluated grinding process of granites using physico-mechanical and mineralogical properties, further illustrating the relationship between rock characteristics and grinding behaviors. Aras et al<sup>3</sup> found

correlations between Bond's parameters and point load index. Zhang et al<sup>20</sup> analyzed the influence of Cerchar Abrasiveness Index on particle size distribution during ball milling, highlighting the potential of using grinding data to understand rock abrasiveness behavior. Aras et al<sup>4</sup> successfully used ANNs to predict Bond work index from rock mechanics properties, demonstrating the potential of machine learning approaches.

To capture the complex behavior during ball mill grinding, Umucu et al<sup>17</sup> employed ANNs to evaluate the grinding process illustrating the importance of material properties. Fuerstenanu et al<sup>9</sup> simulated grinding of coarse/fine (heterogenous) systems in a ball mill providing insights into the complexities involved in grinding process and the potential for using this data to infer rock properties.

Asghari et al<sup>5</sup> investigated the relationship among operational parameters, ore characteristics and product shape properties in an industrial semi-autogenous grinding (SAG) mill further illustrating the interdependence of various factors affecting the grinding process and the potential for using this data to infer rock properties. An investigation was performed by Kecec et al<sup>13</sup> to study the effect of textural properties of rocks on their crushing and grinding characteristics, highlighting the importance of considering rock properties beyond just strength and hardness when analyzing the grinding behavior.

In the domain of rock strength prediction, there is a notable gap in the literature regarding the utilization of grinding characteristics of mills as an indirect approach to correlate with rock properties. Consequently, a study was undertaken to leverage the grinding characteristics of ball mill such as feed input, grinding media quantity, grinding media weight, grind duration, fraction of mill volume occupied by bulk rock charge, fraction of mill volume occupied by bulk ball charge, interstitial filling ratio, charge ratio, extent of mill filling and the characteristics of particle size distribution such as representative particle sizes, width of particle size distribution and steepness factor as predictor variables to predict the uniaxial compressive strength and tensile strength of limestone and granite rocks, using multivariate regression technique.

It is important to note that while ball milling itself is destructive, the ability to predict the rock properties from grinding characteristics eliminates the need for extensive sample preparation and destructive testing typically required for direct methods. A brief overview of multivariate regression method for predicting uniaxial compressive strength model for regression is discussed as follows:

**Multivariate Regression (MVR):** Multivariate regression is used to account for the variance in an interval-dependent, based on linear combinations of interval, dichotomous or dummy-independent variables. It involves a model with one dependent variable and multiple independent variables. The

goal of MVR is to investigate the relationship between multiple independent variables or predictors and a dependent variable or target. Let 'n' be independent variables and 'm' be observations. X denoted the matrix representation of independent variables which is m x (n+1) matrix. The first column of X is typically all ones, representing the intercept term. The dependent variable vector 'y' is m x 1 column vector. The MVR can be represented as shown in eq. 1:

$$y = X\beta + \varepsilon \quad (1)$$

where  $\beta$  is the vector of regression coefficients and  $\varepsilon$  is the vector of errors.

The regression coefficients are typically obtained using least squares method. It is important to acknowledge that while least squares method is effective under certain conditions, it may yield unreliable results under others. A fundamental assumption is that the dependent variable 'y' follows a normal distribution. When the underlying data distribution deviates significantly from normality, the least squares method may produce unreliable results.

## Material and Methods

Field visits were conducted to collect limestone and granite samples from various mines located in different geographical regions in India. These samples were then transported to the laboratory and were prepared to determine uniaxial compressive strength and tensile strength as per ISRM suggested methods. The prepared samples for test are standard NX size with a length-to-diameter ratio of 2.5 for UCS and diameter-to-thickness ratio of 0.5 for TS. In this study, a total of 32 samples consisting of limestone and granite were tested to determine the uniaxial compressive strength and tensile strength.

To determine UCS, the prepared rock samples were centrally aligned on the loading platen and a constant loading rate was applied while recording the applied load until failure occurred. The set up to determine uniaxial compressive strength is shown in figure 1.

For TS determination, an indirect tensile strength test following the Brazilian method was deployed which is represented in figure 2. This involved loading a disc shaped rock specimen along its axis within a diametrical plane. The sample was loaded steadily and consistently until it reached the point of failure, characterized by the initiation of cracks originating from the central region of the disc. The corresponding UCS and TS values were then determined using the load at failure and cross-sectional dimensions. The laboratory test results for UCS and TS samples are shown in table 1.

**Ball mill grinding tests:** For ball mill grinding, the rock specimens of an approximate size of 50-60 mm were initially crushed in a jaw crusher. Subsequently, the crushed material underwent sieving to achieve a size range of -10+6.3 mm.

The obtained sieved rock charge serves as the feed input to the ball mill. Grinding experiments were carried out using a

traditional laboratory-scale ball mill with a total volume of 0.0865 m<sup>3</sup>.

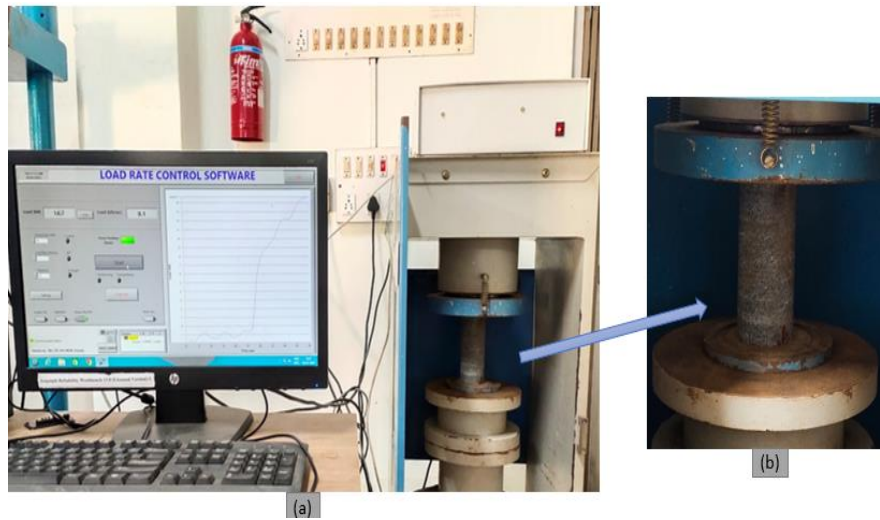


Figure 1: Determination of uniaxial compressive strength (a) Experimental setup (b) Specimen in loading window.

Table 1  
Laboratory test results of uniaxial compressive strength and tensile strength of limestone and granite

Sample	Uniaxial compressive strength (MPa)	Tensile strength (MPa)
Limestone	53.91	6.43
Limestone	53.42	6.37
Limestone	70.41	8.52
Limestone	72.34	10.27
Limestone	84.22	10.30
Limestone	87.61	10.74
Limestone	57.28	6.85
Limestone	46.51	5.50
Limestone	84.75	10.37
Limestone	91.75	11.27
Limestone	93.80	11.54
Limestone	86.01	10.53
Limestone	98.02	12.09
Limestone	122.54	15.30
Limestone	97.59	12.03
Limestone	93.75	11.53
Granite	80.32	11.50
Granite	82.45	12.86
Granite	111.57	21.54
Granite	148.00	26.77
Granite	88.15	11.74
Granite	75.00	10.41
Granite	126.64	21.01
Granite	129.74	22.14
Granite	111.24	16.45
Granite	120.41	19.78
Granite	108.90	15.42
Granite	103.12	17.16
Granite	93.562	16.8
Granite	108.66	17.32
Granite	127.85	18.41
Granite	133.00	23.34



**Figure 2: Experimental setup for Brazilian tensile strength test (a) Brazilian apparatus to conduct the test (b) Rock specimen before the failure (c) Crack propagation under tensile loading (d) Rock specimen after the failure**



**Figure 3: A view of laboratory ball mill**

A typical laboratory ball mill is shown in figure 3. The mill operates at a speed of 55 rpm, which is 70% of its critical speed. To facilitate the grinding process, an adequate amount of grinding medium (HCHC balls having density = 7.45 g/cc) is added to the ball mill drum. For the dry grinding experiments, the test sample's volume is selected so that the combined volume of the sample and grinding media is less than 40% of the total mill volume. The grinding characteristics of ball mill including the operating parameters are shown in table 2, table 3 and particle size distribution characteristics are shown in table 4 and table 5 for limestone and granite samples. The representative particle sizes of the particle size distribution considered in this study are:  $d_{10}$ ,  $d_{20}$ ,  $d_{50}$ ,  $d_{80}$ ,  $d_{84}$  and  $d_{90}$  in  $\mu\text{m}$ . Also, the two measures of particle size distribution are steepness factor (SF) and width of particle size distribution (WPSD).

Certain parameters of the ball mill such as fraction of mill volume occupied by bulk rock charge ( $J_r$ ), fraction of mill volume occupied by bulk ball charge ( $J_b$ ), interstitial filling ratio (U), charge ratio ( $\nu$ ), extent of mill filling ( $\psi$ ), steepness factor (SF), width of particle size distribution (WPSD) are determined using the expressions shown in eq. 2 to 8:

$$J_r = \frac{m_r}{\rho_r} * \frac{100}{V_{\text{mill}} (1 - \epsilon)} \quad (2)$$

$$J_b = \frac{m_b}{\rho_b} * \frac{100}{V_{\text{mill}} (1 - \epsilon)} \quad (3)$$

$$\omega = \frac{J_r}{J_b} * \frac{1}{\epsilon} \quad (4)$$

$$\nu = \frac{m_b}{m_r} \quad (5)$$

$$\psi = \frac{\left(\frac{m_r}{\rho_r} + \frac{m_b}{\rho_b}\right)}{V_{\text{mill}}} * \frac{100}{1 - \epsilon} \quad (6)$$

$$\text{SF} = \frac{d_{50}}{d_{20}} \quad (7)$$

$$\text{WPSD} = \frac{(d_{90} - d_{10})}{d_{50}} \quad (8)$$

where  $m_r$  is the mass of rock charge,  $m_b$  is the mass of balls charge,  $\rho_r$  is density of rock charge,  $\rho_b$  is density of ball charge ( $\rho_b = 7.65 \text{ g/cc}$ ),  $V_{\text{mill}}$  is the mill volume and  $\epsilon$  is bed porosity for ball mill (30-40%) while  $d_{10}$ ,  $d_{20}$ ,  $d_{50}$ ,  $d_{80}$ ,  $d_{84}$  and  $d_{90}$  are the sieve sizes having 10%, 20%, 50%, 80%, 84% and 90% cumulative weight passing size in  $\mu\text{m}$ .

Steepness factor is a measure of the slope of the particle size distribution curve and it is defined as the ratio of the particle size corresponding to 50% passing ( $d_{50}$ ) to the particle size corresponding to 20% passing ( $d_{20}$ ). If SF is more than two, then the particle size distribution is broader in range and if

SF is less than two, the particle size distribution is narrower or steeper in range<sup>14</sup>. The SF for the ground materials varied from 2.67 to 5.41 for limestone and 2.78 to 4.33 for granite which clearly indicates broader particle size distribution.

Width of particle size distribution, on the other hand, refers to the range of particle sizes present in the distribution and it can be measured using different parameters such as the range, standard deviation, variance and coefficient of variation. A narrow width of particle size distribution indicates that most of the particles are of similar size while a wide width indicates a broad range of particle sizes. In this study, the width of particle size distribution is taken as relative span or coefficient of variation ( $CV = (d_{90} - d_{10}) / d_{50}$ ) which is a dimensionless measure of PSD. For limestone the

WPSD varies between 11.11 to 19.29 whereas for granite, it varies between 14.03 to 22.77.

**Results and Discussion**

The development of the prediction models for predicting uniaxial compressive strength and tensile strength of rocks from grinding characteristics of ball mill, performance evaluation of developed models and validation of developed prediction models are discussed.

**Predictive modeling of uniaxial compressive strength and tensile strength:** Multivariate regression is carried out to develop the prediction models for UCS and TS using the grinding characteristics of ball mill as independent variables.

**Table 2**  
**Operating parameters of ball mill for limestone grinding**

Test Run	FI	GMQ	GMW (kg)	J <sub>r</sub> (%)	J <sub>b</sub> (%)	U	τ (min)	v	Ψ (%)
1	1000	125	16.74	0.70	3.91	0.49	300	16.74	4.88
2	1000	135	19.39	0.69	4.53	0.42	450	19.39	5.54
3	1000	145	23.57	0.71	5.50	0.36	600	23.57	6.59
4	1000	155	28.85	0.69	6.74	0.28	750	28.85	7.90
5	1250	125	23.20	0.87	5.42	0.44	450	18.56	6.67
6	1250	135	25.76	0.85	6.01	0.39	300	20.61	7.29
7	1250	145	31.01	0.86	7.24	0.33	750	24.81	8.61
8	1250	155	34.21	0.82	7.99	0.28	600	27.37	9.39
9	1500	125	23.33	1.00	5.45	0.51	600	15.55	6.86
10	1500	135	27.51	1.03	6.42	0.44	750	18.34	7.91
11	1500	145	29.90	0.98	6.98	0.39	300	19.93	8.49
12	1500	155	33.37	1.07	7.79	0.38	450	22.25	9.37
13	1750	125	25.80	1.19	6.03	0.54	750	14.74	7.64
14	1750	135	28.84	1.17	6.73	0.48	600	16.48	8.40
15	1750	145	33.29	1.18	7.77	0.42	450	19.02	9.50
16	1750	155	37.37	1.17	8.73	0.37	300	21.35	10.51

**Table 3**  
**Operating parameters of ball mill for granite grinding**

Test Run	FI	GMQ	GMW (kg)	J <sub>r</sub> (%)	J <sub>b</sub> (%)	U	τ (min)	v	Ψ (%)
1	1000	125	15.924	0.626	3.979	0.437	5.0	15.924	4.718
2	1000	135	17.093	0.686	4.271	0.446	7.5	17.093	5.079
3	1000	145	23.972	0.664	5.990	0.308	10.0	23.972	6.825
4	1000	155	29.112	0.670	7.274	0.256	12.5	29.112	7.337
5	1250	125	22.822	0.839	5.703	0.409	7.5	18.258	6.704
6	1250	135	20.391	0.826	5.095	0.450	5.0	16.313	7.198
7	1250	145	24.576	0.773	6.141	0.350	12.5	19.661	7.089
8	1250	155	30.528	0.834	7.628	0.304	10.0	24.422	8.680
9	1500	125	19.335	0.946	4.831	0.544	10.0	12.890	5.916
10	1500	135	22.615	0.999	5.651	0.491	12.5	15.077	6.811
11	1500	145	26.809	1.044	6.699	0.433	5.0	17.873	7.935
12	1500	155	34.738	1.027	8.680	0.329	7.5	23.159	9.955
13	1750	125	20.446	1.245	5.109	0.677	12.5	11.683	6.500
14	1750	135	23.418	1.268	5.852	0.602	10.0	13.382	7.287
15	1750	145	26.811	1.195	6.699	0.495	7.5	15.321	8.086
16	1750	155	38.225	1.061	9.551	0.309	5.0	21.843	10.886

**Table 4**  
**Characteristics of particle size distribution of limestone**

Test Run	d <sub>10</sub> (µm)	d <sub>20</sub> (µm)	d <sub>50</sub> (µm)	d <sub>80</sub> (µm)	d <sub>84</sub> (µm)	d <sub>90</sub> (µm)	SF	WPSD
1	44.13	82.34	445.53	2657.70	3869.60	5205.59	5.41	11.59
2	43.11	87.43	450.58	2140.33	3795.20	5226.98	5.15	11.50
3	40.21	89.83	385.77	2518.75	3782.54	5157.14	4.29	13.26
4	43.89	85.99	317.23	2459.77	3801.36	4885.46	3.69	15.26
5	46.31	90.04	356.52	2089.51	3672.70	5181.99	3.96	14.41
6	53.23	92.98	365.67	2086.93	3821.49	5096.39	3.93	13.79
7	39.73	90.23	384.44	1935.29	3591.72	5080.51	4.26	13.11
8	47.69	95.41	438.66	2743.57	3166.27	4921.73	4.60	11.11
9	53.43	90.55	318.13	2200.96	2928.96	4811.42	3.51	14.96
10	46.72	87.62	326.75	1976.88	3600.25	4979.18	3.73	15.10
11	51.85	96.40	360.74	2285.21	3393.73	5167.12	3.74	14.18
12	44.72	90.16	412.09	2193.57	3773.63	5300.00	4.57	12.75
13	45.84	88.38	313.13	2296.44	3476.12	5001.21	3.54	15.83
14	48.85	92.27	246.54	2134.72	3100.23	4804.55	2.67	19.29
15	51.00	93.55	279.44	2153.50	3192.69	4832.14	2.99	17.11
16	52.55	95.71	429.85	2190.10	3300.90	5017.25	4.49	11.55

**Table 5**  
**Characteristics of particle size distribution of granite**

Test Run	d <sub>10</sub> (µm)	d <sub>20</sub> (µm)	d <sub>50</sub> (µm)	d <sub>80</sub> (µm)	d <sub>84</sub> (µm)	d <sub>90</sub> (µm)	SF	WPSD
1	45.38	67.60	281.23	3365.02	4486.35	5416.83	4.16	19.10
2	43.49	71.20	303.52	3645.29	4175.56	5331.95	4.26	17.42
3	42.99	69.44	279.01	3247.94	4397.62	5327.96	4.02	18.94
4	40.88	74.69	300.34	3419.90	4421.02	5302.70	4.02	17.52
5	45.30	71.83	225.38	3017.42	4108.22	5177.85	3.14	22.77
6	52.09	80.32	244.85	2870.84	3794.15	5112.75	3.05	20.67
7	44.91	75.33	292.66	3168.54	4200.23	5200.12	3.89	17.62
8	42.22	70.31	274.57	3302.92	4043.62	5160.95	3.91	18.64
9	49.54	70.57	284.70	2939.48	3704.84	5210.36	4.03	18.13
10	48.39	77.23	276.31	3097.05	3897.42	5150.69	3.58	18.47
11	50.54	83.96	252.07	2198.08	3441.09	5011.87	3.00	19.68
12	45.61	82.22	355.72	2677.60	3903.17	5037.89	4.33	14.03
13	45.24	73.90	249.52	3173.16	4030.41	5220.45	3.38	20.74
14	47.32	77.38	252.58	2671.79	3571.23	5135.64	3.26	20.15
15	52.87	87.66	263.55	2050.54	3298.21	4896.33	3.01	18.38
16	48.88	80.51	223.68	2811.63	3829.97	5100.20	2.78	22.58

In this study, the grinding characteristics of the ball mill include feed input, grinding media quantity i.e., number of balls, grinding media weight, fraction of mill volume occupied by the bulk rock charge, fraction of mill volume occupied by the bulk ball charge, interstitial filling ratio, grinding duration, charge ratio, extent of mill filling, representative cumulative weight passing sieve sizes in microns respectively. The developed models are shown in eq. 9 and 10.

$$\begin{aligned}
 \text{UCS (MPa)} = & -576.93 + 0.15\text{FI} - 0.056\text{GMQ} - 0.017\text{GMW} \\
 & + 111.95\text{J}_r + 55.37\text{J}_b - 472.93\text{U} + 136.56\tau + 6.99\nu - 19.32\psi \\
 & + 0.23\text{d}_{10} + 4.35\text{d}_{20} - 1.38\text{d}_{50} + 0.01\text{d}_{80} - 0.008\text{d}_{84} + 0.07\text{d}_{90} \\
 & + 82.31\text{SF} - 0.73\text{WPSD} - 153.73\text{U}^2 + 0.94\text{U} * \text{d}_{50} \quad (9)
 \end{aligned}$$

$$\begin{aligned}
 \text{TS (MPa)} = & -295.55 + 0.02\text{FI} + 0.03\text{GMQ} - 0.005\text{GMW} - \\
 & 19.22\text{J}_r + 21.99\text{J}_b - 8.26\text{U} + 73.93\tau + 0.59\nu - 1.76\psi + \\
 & 1.81\text{d}_{10} + 0.93\text{d}_{20} - 0.23\text{d}_{50} - 0.002\text{d}_{80} - 0.003\text{d}_{84} + 0.01\text{d}_{90} \\
 & + 22.74\text{SF} + 0.61\text{WPSD} - \tau^2 1185.14 - 335.40\tau^2 * \text{SF} \quad (10)
 \end{aligned}$$

where FI is feed input, GMQ is grinding media quantity, GMW is grinding media weight, J<sub>r</sub> is the fraction of mill volume occupied by bulk rock charge, J<sub>b</sub> is the fraction of mill volume occupied by bulk ball charge, U is interstitial filling ratio, τ is grinding duration, ν is charge ratio, ψ is extent of mill filling and d<sub>10</sub>, d<sub>20</sub>, d<sub>50</sub>, d<sub>80</sub>, d<sub>84</sub> and d<sub>90</sub> are the sieve sizes having 10%, 20%, 50%, 80%, 84% and 90% cumulative weight passing sizes in µm, WPSD and SF are the widths of the particle size distribution and steepness

factor. The model summary for models UCS and TS are shown in table 6.

Correlation between the grinding characteristics of ball mill and uniaxial compressive strength (UCS) for different types of rocks is evaluated with aid of regression models. Multivariate dependence techniques have their main objective to specify a model that can explain and predict the behaviour of one or more dependent variables through one or more explanatory variables. A multivariate regression considers the effect of more than one explanatory variable on some outcome of interest. It evaluates the relative effect of these explanatory, or independent, variables on the dependent variable when holding all the other variables in the model constant.

The residuals plot for UCS including normal probability plot, residual versus fit, histogram and residuals versus order is shown in figure 4. The minimum and maximum residuals values obtained for the prediction model UCS are -9.56 MPa and 16.53 MPa. The standard deviations in the predicted value and residuals are found to be 23.18 and 6.13

respectively. A plot between actual and predicted UCS values from the multivariate regression model UCS is shown in figure 5. The predicted UCS ranged from 51.75 to 143.89 MPa. The mean of the predicted value for UCS of rocks is 95.37 MPa. The overall trend was upwards, with the natural fluctuations stimulated from the prediction model. The correlogram for dependent variable UCS with grinding characteristics is shown in figure 6.

The correlation matrix shows the relationships among the grinding characteristics of ball mill and also with UCS dependent variable. The median particle size was found to have a higher inverse correlation with UCS. The operating parameters have lower influence whereas the characteristics of particle size distribution have higher correlation with UCS. Similarly, the prediction model is developed for tensile strength using grinding characteristics as input variables and the model summary is shown in table 6. The correlation coefficient for the developed model is 0.965. The residuals plot for tensile strength of rocks is shown in figure 7. The minimum and maximum residuals values are -1.56 MPa and 2.35 MPa with a standard deviation of 1.01.

**Table 6**  
**Model summary of UCS and TS**

Model	R	R <sup>2</sup>	Adjusted R <sup>2</sup>	Std. Error of the Estimate
UCS	0.96	0.93	0.93	1.86
TS	0.98	0.96	0.90	1.62

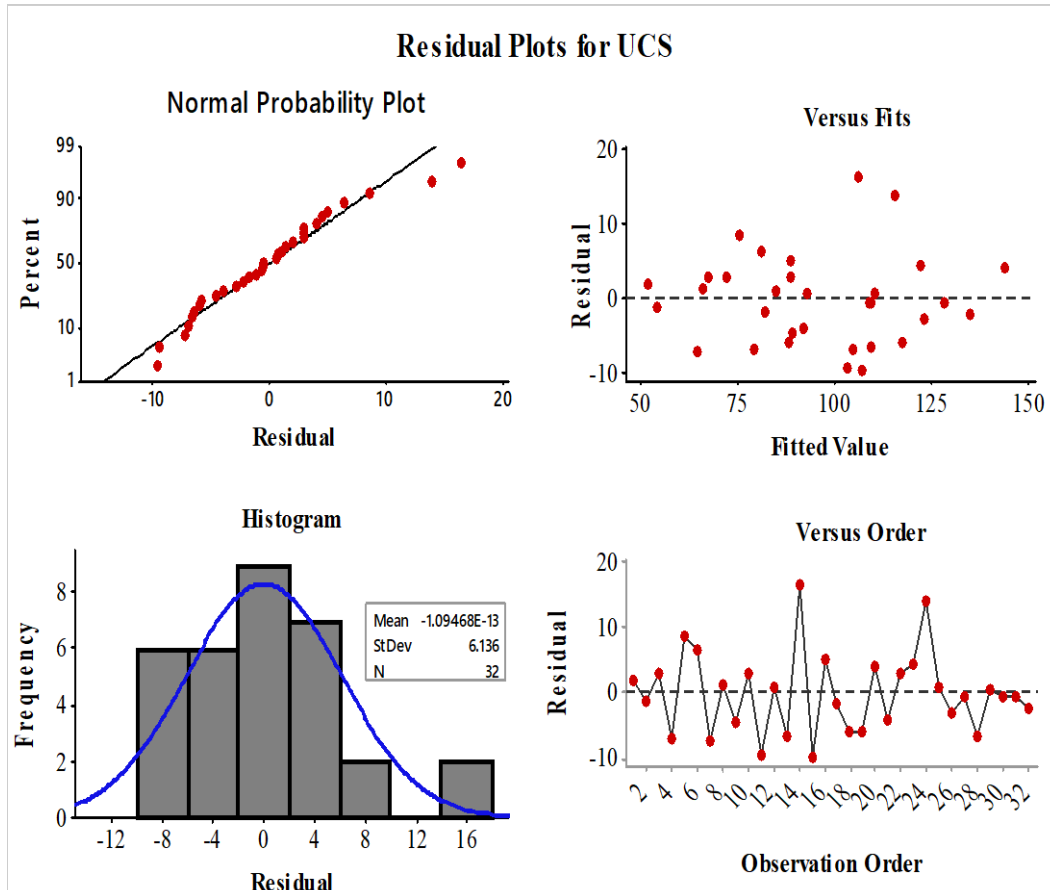


**Figure 4: Residual plots of UCS model**

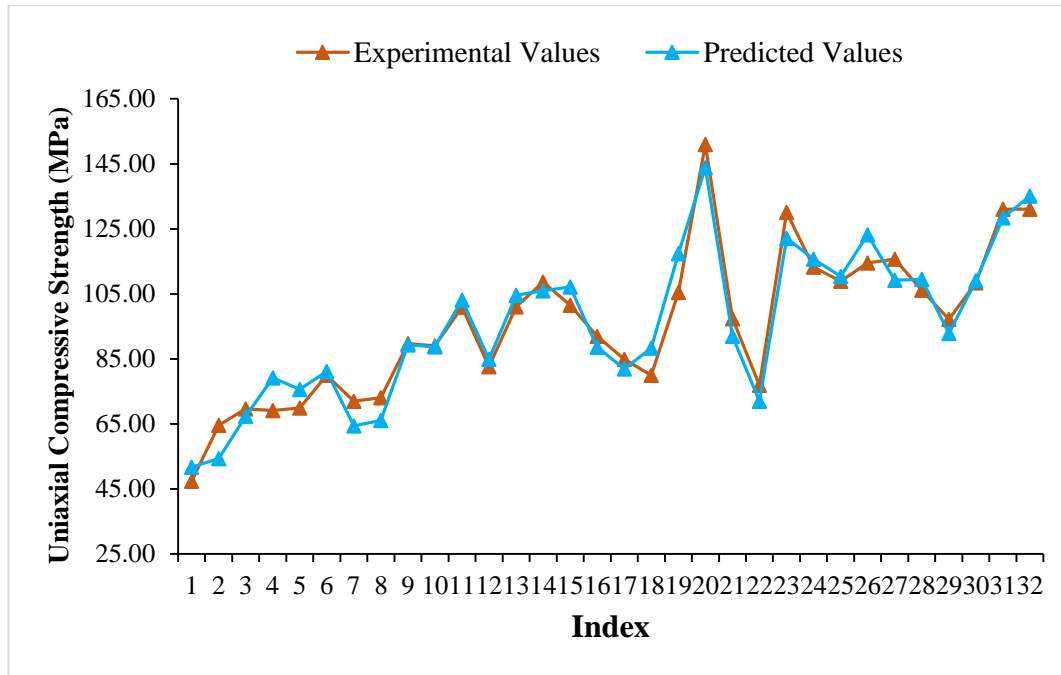


Figure 5: A plot of predicted and experimental uniaxial compressive strength

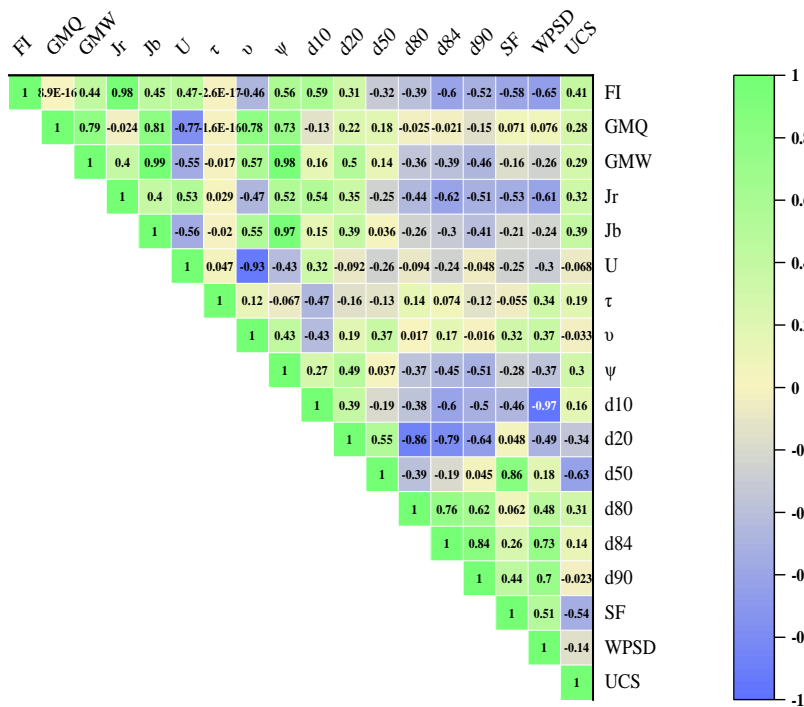


Figure 6: Correlogram between uniaxial compressive strength and the grinding characteristics

The normal probability plot of the residuals verifies the assumption that the residuals are normally distributed. The residuals versus fits plot shown in figure 7 validates the assumption that residuals are randomly distributed and have constant variance. A plot between the experimental and predicted values of tensile strength is shown in figure 8. The mean of the predicted value for tensile strength of rocks is 13.82 MPa with a standard deviation of 5.27.

The correlogram between tensile strength and grinding characteristics is shown as in figure 9. The correlation matrix

shows the relationships among the grinding characteristics of ball mill and also with TS dependent variable. Similar to UCS, the median particle size was found to have a higher inverse correlation with TS. The operating parameters have lower influence and vice versa for representative particle.

**Performance evaluation of prediction models:** One of the crucial steps in the development of a prediction model is the assessment of model based on performance indices which reports its validity for prediction. A few commonly used metrics for evaluating the performance of MVR models

include coefficient of determination ( $R^2$ ), root mean square error (RMSE) and variance accounted for (VAF) and they are shown in eq. 11 to 13.  $R^2$  quantifies the strength and direction of linear relationship between the two variables. RMSE reflects the standard deviation of residuals. VAF measures the proportion of error variance relative to the variance in the observed data. According to Hair et al<sup>10</sup>, a  $VAF > 80\%$  indicates full mediation, between 20% and 80% suggests partial mediation and  $< 20\%$  implies no mediation.

$$R^2 = 1 - \frac{\sum_i(y_a - y_p)^2}{\sum_i(y_a - y_m)^2} \tag{11}$$

$$RMSE = \sqrt{\frac{1}{N} \sum_{i=1}^N (y_p - y_a)^2} \tag{12}$$

$$VAF = \left(1 - \frac{var(y_a - y_p)}{var(y_a)}\right) * 100 \tag{13}$$

where  $N$  is represents the number of samples,  $y_a$  is represents the true value or actual value,  $y_p$  is represents the predicted values and  $y_m$  is represents mean value.

The calculated performance indices for the developed regression models UCS and TS are shown in table 7. For an excellent prediction model with high level of acceptability, in theory, the  $R^2$ , RMSE and VAF will have the values of 1, 0 and 100% respectively<sup>8</sup>.

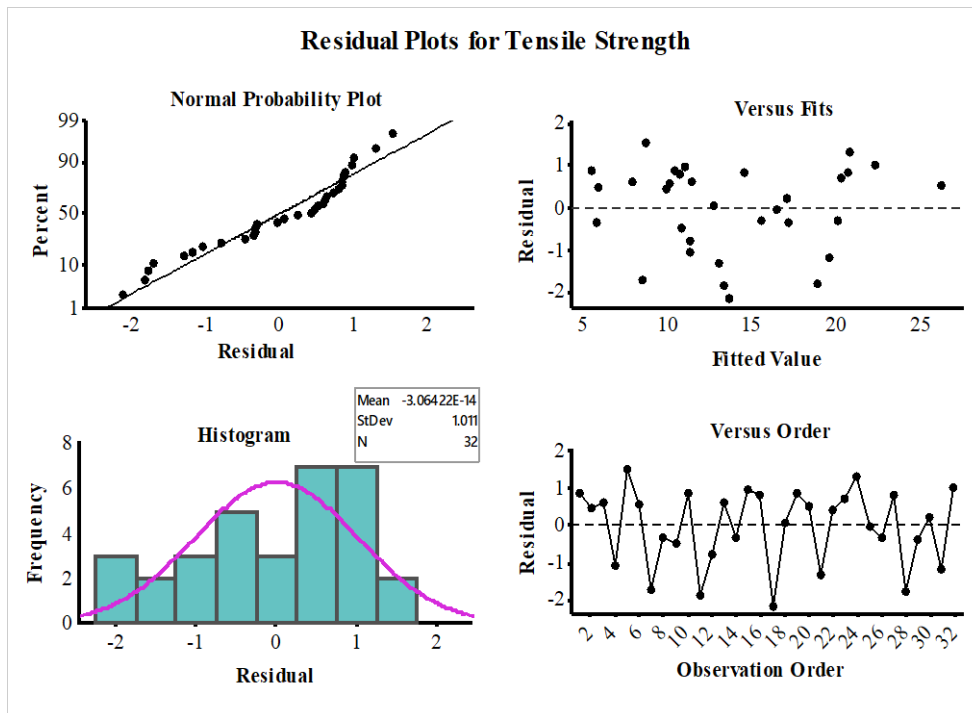


Figure 7: Residual plots of TS model

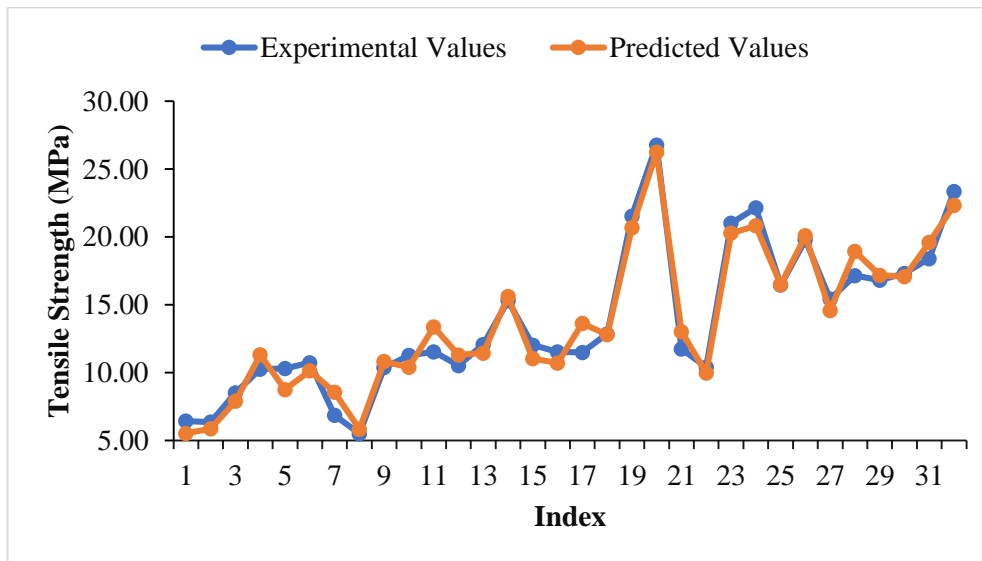


Figure 8: A plot of predicted and experimental tensile strength

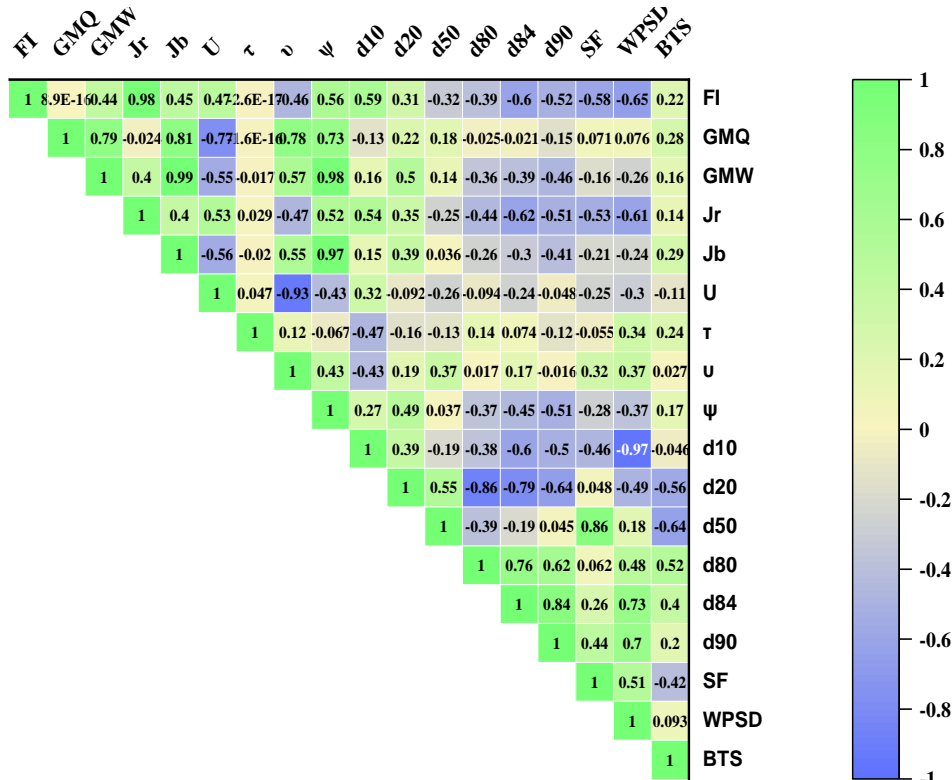


Figure 9: Correlogram between tensile strength and grinding characteristics

Table 7  
Performance evaluation metrics for developed prediction models

Prediction Model (Dependent Variable)	Performance Evaluation Indexes		
	R <sup>2</sup>	RMSE	VAF (%)
UCS	0.93	6.03	93.45
TS	0.96	0.99	96.47

Table 8  
Physico-mechanical properties of basalt rocks

Rock	Uniaxial Compressive Strength, MPa	Tensile Strength, MPa
Basalt	158.52	5.85
	55.56	7.01
	138.07	6.23

**Validation of the developed prediction models:** The proposed prediction models are validated by predicting the uniaxial compressive strength and tensile strength of basalt rocks (for the present study). The test data is gathered by conducting batch grinding tests on basalt rocks to generate the grinding characteristics of the ground sample. Laboratory tests are conducted to determine the UCS and TS as shown in table 8. The table 9 provide the test conditions for ball mill grinding of rock samples under dry conditions.

The density of grinding media is 7.65 g/cc made of high chrome high carbon steel balls. A bed porosity ( $\epsilon$ ) of 0.36 is assumed for the ball mill. The particle size distribution is obtained after sieving the ground product for a duration of 10 minutes and the representative cumulative weight

percentage passing sieve sizes are calculated and the corresponding characteristics of particle size distribution are obtained. Table 10 provides the particle size distribution for the ground basalt samples. The operating parameters of ball mill and characteristics of particles size distribution of ground samples generated account for validation which serves as inputs to predict the UCS and TS of basalt. The predicted UCS and TS models are tabulated and compared with the experimental values.

The change in true value and predicted value yields the associated error or residual of the prediction model and henceforth error percentage is calculated. A large error signifies the poor prediction model. The validations of models are shown in table 11.

**Table 9**  
**Operational parameters of ball mill for grinding of basalt samples**

Parameters	Values
Feed input to ball mill (g)	500, 600, 700
Grinding media	40, 55, 70
Grinding media weight (kg)	6.957, 8.456, 10.050
Grinding duration (min)	5.0, 10.0, 15.0
Bulk rock charge fraction (%)	0.39, 0.42, 0.51
Bulk ball charge fraction (%)	1.63, 1.99, 2.36
Interstitial filling ratio	0.67, 0.58, 0.59
Charge ratio	13.91, 14.90, 14.35
Extent of mill filling (%)	2.03, 2.41, 2.87
Feed input to ball mill (g)	500, 600, 700

**Table 10**  
**Characteristics of particle size distribution of basalt samples**

S.N.	Particle Size Distribution							
	d <sub>10</sub>	d <sub>20</sub>	d <sub>50</sub>	d <sub>80</sub>	d <sub>84</sub>	d <sub>90</sub>	SF	WPSD
1	55.76	104.23	430.24	1910.27	2552.11	4022.21	7.71	72.13
2	48.12	90.21	368.49	1750.53	2498.22	3815.81	7.65	79.28
3	43.21	85.30	315.51	1530.12	2304.43	3666.91	7.30	84.85

**Table 11**  
**Validation of developed prediction models**

Prediction Model	Actual Values	Predicted Values	Error Percentage
UCS (MPa)	158.52	140.11	11.61
	55.56	49.63	10.68
	138.07	131.02	5.10
TS (MPa)	5.85	5.60	4.26
	7.01	6.17	12.30
	6.21	5.19	16.39

Slightly higher error percentages are observed for uniaxial compressive strength prediction model. Prediction models are dominated by large data size. Insufficient data available in the development of prediction models may results in higher prediction errors.

### Conclusion

Numerous researchers have investigated various indirect methodologies for estimating rock properties. Directly assessing these properties in rock engineering projects proves intricate and time-consuming. This study introduces an innovative approach that utilizes the grinding characteristics of a ball mill to predict uniaxial compressive strength and tensile strength. Predictive modelling is performed to establish the correlations between UCS, TS and grinding characteristics of the ball mill. The model accuracy is assessed based on  $R^2$  for the developed prediction model with  $R^2$  values of 0.93 for UCS and 0.96 for TS.

Performance evaluation metrics are applied to assess the performance of prediction models, showing an RMSE of 6.03 MPa and VAF of 93.45% for UCS and an RMSE of

0.994 MPa and VAF of 96.47% for TS. To validate the developed prediction models, UCS and TS of basalt rocks and the results of ball mill grind tests are used and the error percentage is estimated for the predicted and experimental values of basalt rock properties. The error percentage for UCS varied from 5.1% to 11.61%, while for TS it varied between 4.26% to 16.39% respectively. The proposed models demonstrate good accuracy, indicating their robustness and reliability.

However, the current scope of these models is limited to a small selection of rock types. To fully establish their generalizability, a comprehensive investigation encompassing a broader range of rock types and a more diverse dataset is essential. Such an expansion would enhance the predictive capability of the models and would solidify their potential for widespread applications in rock mechanics and rock engineering.

### References

1. Abdel Hafeez G.S., Correlation between bond work index and mechanical properties of some Saudi ores, *JES Journal of Engineering Sciences*, **40(1)**, 271–80 (2012)

2. Ahmadi Sheshde E. and Cheshomi A., New method for estimating unconfined compressive strength (UCS) using small rock samples, *J. Petroleum Science and Engg.*, **133**, 367–75 (2015)
3. Aras A., Ozkan A. and Aydogan S., Correlations of Bond and breakage parameters of some ores with the corresponding point load index, *Particle & Particle Systems Characterization*, **29(3)**, 204–10 (2012)
4. Aras A., Aras A., Özşen H. and Dursun A.E., Using Artificial Neural Networks for the Prediction of Bond Work Index from Rock Mechanics Properties, *Mineral Processing and Extractive Metallurgy Review*, **41(3)**, 145–52 (2020)
5. Asghari M., Vand Ghorbany O. and Nakhaei F., Relationship among operational parameters, ore characteristics and product shape properties in an industrial SAG mill, *Particulate Science and Technology*, **38(4)**, 482–93 (2020)
6. Bearman R.A., Briggs C.A. and Kojovic T., The applications of rock mechanics parameters to the prediction of comminution behaviour, *Minerals Engineering*, **10(3)**, 255–64 (1997)
7. Cemiloglu A. et al, Support vector machine (SVM) application for uniaxial compression strength (UCS) prediction: A case study for Maragheh Limestone, *Applied Sciences*, **13(4)**, 2217 (2023)
8. Ceryan N., Okkan U. and Kesimal A., Prediction of unconfined compressive strength of carbonate rocks using artificial neural networks, *Environ. Earth Sciences*, **68(3)**, 807–19 (2013)
9. Fuerstenau D.W., Phatak P.B., Kapur P.C. and Abouzeid A.Z.M., Simulation of the grinding of coarse/fine (heterogeneous) systems in a ball mill, *Int. J. Mineral Processing*, **99(1–4)**, 32–8 (2011)
10. Hair J.F., Ringle C.M. and Sarstedt M., PLS-SEM: Indeed, a Silver Bullet, *J. Marketing Theory and Practice*, **19(2)**, 139–52 (2011)
11. Hatheway A.W., The complete ISRM suggested methods for rock characterization, testing and monitoring; 1974–2006, *Environ & Engg. Geosci.*, **15(1)**, 47–8 (2009)
12. Kahraman S., Ucurum M., Yogurtcuoglu E. and Fener M., Evaluating the grinding process of granites using the physico-mechanical and mineralogical properties, *J. Metals, Materials and Minerals*, **29(2)**, 51–7 (2019)
13. Kecec B., Unal M. and Sensogut C., Effect of the textural properties of rocks on their crushing and grinding features, *J. Univ. Science and Technology Beijing*, **13(5)**, 385–92 (2006)
14. Öksüzöğlü B. and Uçurum M., An experimental study on the ultra-fine grinding of gypsum ore in a dry ball mill, *Powder Tech.*, **291**, 186–92 (2016)
15. Parsajoo M., Armaghani D.J., Mohammed A.S., Khari M. and Jahandari S., Tensile strength prediction of rock material using non-destructive tests: A comparative intelligent study, *Transportation Geotech.*, **31**, 100652 (2021)
16. Petrakis E. and Komnitsas K., Correlation between material properties and breakage rate parameters determined from grinding tests, *Applied Sciences*, **8(2)**, 220 (2018)
17. Umucu Y., Deniz V., Bozkurt V. and Fatih Çallar M., The evaluation of grinding process using artificial neural network, *Int. J. Mineral Processing*, **146**, 46–53 (2016)
18. Wei X., Shahani N.M. and Zheng X., Predictive modeling of the uniaxial compressive strength of rocks using an artificial neural network approach, *Mathematics*, **11(7)**, 1650 (2023)
19. Yang H.Q., Li Z., Jie T.Q. and Zhang Z.Q., Effects of joints on the cutting behavior of disc cutter running on the jointed rock mass, *Tunnelling and Underground Space Technology*, **81**, 112–20 (2018)
20. Zhang S., Zhou Z., Gao Z., Cai X. and Song W., Analyzing the influence of Cerchar abrasiveness index on particle size distribution in ball milling based on multifractal theory, *Powder Tech.*, **429**, 118947 (2023).

(Received 22<sup>nd</sup> January 2025, accepted 20<sup>th</sup> February 2025)